Extending the Range of the Inductionless Magnetorotational Instability

Oleg N. Kirillov[*] and Frank Stefani[†]

Helmholtz-Zentrum Dresden-Rossendorf, P.O. Box 510119, D-01314 Dresden, Germany

The magnetorotational instability (MRI) can destabilize hydrodynamically stable rotational flows, thereby allowing angular momentum transport in accretion disks. A notorious problem for the MRI is its questionable applicability in regions with low magnetic Reynolds number. Using the WKB method, we extend the range of applicability of the MRI by showing that the inductionless versions of the MRI, such as the helical MRI and the azimuthal MRI, can easily destabilize Keplerian profiles $\propto r^{-3/2}$ if the radial profile of the azimuthal magnetic field is only slightly modified from the current-free profile $\propto r^{-1}$. This way we further show how the formerly known lower Liu limit of the critical Rossby number Ro ≈ -0.828 connects naturally with the upper Liu limit Ro $\approx +4.828$.

Initiated by the seminal work of Balbus and Hawley [1], the magnetorotational instability (MRI) has become the standard explanation for turbulence and enhanced angular momentum transport in accretion disks around black holes and protostars. While the MRI is thought to be a robust phenomenon in the hot parts of accretion disks, a notorious problem concerns the viability of the MRI in other regions, such as the outer parts of black hole accretion disks [2] and the ''dead zones'' of protoplanetary disks [3]. This has to do with the fact that the onset of the MRI demands that both the rotation period and the Alfvén crossing time in the vertical direction are shorter than the time scale for magnetic diffusion [4]. For the case of a vertical magnetic field B_z applied to a disk of height H this means that both the magnetic Reynolds number Rm $= \mu_0 \sigma H^2 \Omega$ and the Lundquist number $S = \mu_0 \sigma H v_A$ must be larger than one, and that $S \lesssim$ Rm (Ω is the angular velocity, μ_0 is the magnetic permeability, σ the conductivity, $v_A := B_z/\sqrt{\mu_0 \rho}$ is the Alfvén velocity, with ρ denoting the density). In a disk with given size, angular velocity, and magnetic field strength it is then often the spatially varying magnetic Prandtl number Pm $= \nu/\eta$, i.e., the ratio of viscosity ν to magnetic diffusivity $\eta := (\mu_0 \sigma)^{-1}$, that determines the values of Rm and S, and hence the fate of the MRI.

For the case without an external B_z things are even more complicated since the MRI-triggering magnetic field, in this case dominated by the azimuthal component B_ϕ, must be produced in the disk itself, very likely by some sort of an $\alpha - \Omega$ dynamo [5] or a periodic MRI dynamo process [6]. This combined, looplike action of the MRI and self-excitation has attracted much attention in the past, with many open questions concerning issues of numerical convergence [7], as well as the role of disk stratification [8] and vertical boundary conditions [9]. Again, the most interesting case appears in the limit of low Pm. While Lesur and Longaretti [10] have argued for a power-law decline of the turbulent transport with decreasing Pm, there are also indications for the existence of some critical Rm in the order of $10^3 \dots 10^4$ for the MRI-dynamo loop to work [11].

Exactly this situation, characterized by low Pm and a significant or even dominant B_ϕ, is the subject of intense theoretical and experimental research initiated by Hollerbach and Rüdiger [12]. For the ratio of B_ϕ to B_z being on the order of 1 and $B_\phi(r) \propto 1/r$, the helical MRI (HMRI) was shown to work also in the inductionless limit [13], Pm $= 0$, and to be governed by the Reynolds number Re $=$ RmPm^{-1} and the Hartmann number Ha $= S$Pm$^{-1/2}$, quite in contrast to the standard MRI (SMRI) that is governed by Rm and S.

Somewhat disappointingly, a crucial limitation of this surprising kind of MRI was identified by Liu *et al.* [14] who used a WKB approach to find a minimum steepness of the rotation profile, expressed by the Rossby number Ro $:= r(2\Omega)^{-1}\partial\Omega/\partial r <$ Ro$_{\rm LLL} = 2(1 - \sqrt{2}) \approx -0.828$. This limit, which we call the lower Liu limit (LLL) in the following, implies that the inductionless HMRI in the case when $B_\phi(r) \propto 1/r$ does not extend to the most relevant Keplerian case, characterized by Ro$_{\rm Kep} = -3/4$. In addition to the LLL, the authors found also a second threshold of the Rossby number, which we call the upper Liu limit (ULL), at Ro$_{\rm ULL} = 2(1 + \sqrt{2}) \approx +4.828$. This second limit, which implies a magnetic destabilization of extremely stable flows with strongly increasing angular frequency, has attained nearly no attention up to present, but will play an important role below.

The existence of the LLL, together with a variety of further predicted parameter dependencies, was confirmed in the PROMISE experiment working with a low-Pm liquid metal [15]. Present experimental work at the same device aims at the characterization of the azimuthal MRI (AMRI), a nonaxisymmetric ''relative'' of the axisymmetric HMRI, which is expected to dominate at large ratios of B_ϕ to B_z [16]. However, AMRI as well as inductionless MRI modes

with any integer azimuthal wave number m (which may be relevant at small values of B_ϕ/B_z), seem also to be constrained by the LLL as recently shown in a unified WKB treatment of all inductionless versions of the MRI [17]. Actually, it is the apparent failure of the HMRI, and the AMRI, to apply to Keplerian profiles that has prevented a wider acceptance of those inductionless forms of the MRI in the astrophysical community. Only recently, the intricate, though continuous, transition between the SMRI and the HMRI was explained in some detail by showing that it involves a spectral exceptional point at which the inertial wave branch coalesces with the branch of the slow magneto-Coriolis wave [18].

Given the fundamental importance of whether any sort of inductionless MRI could possibly work in the low-Pm regions of accretion disks, it is quite natural to ask how to extend the range of its applicability beyond the LLL. In a first attempt, the stringency of the LLL for $B_\phi(r) \propto 1/r$ was questioned by Rüdiger and Hollerbach [19] who had found an extension of the LLL to Keplerian values in global simulations when at least one of the radial boundary conditions was assumed electrically conducting. Later, though, by distinguishing between convective and absolute instabilities for the travelling waves such as the HMRI, the LLL was vindicated even for such modified electrical boundary conditions [13]. A second attempt was made in Ref. [20] treating the HMRI for nonzero, but low, S. It was found that for $B_\phi(r) \propto 1/r$, the essential HMRI mode extends from $S = 0$ only to a value $S \approx 0.618$, and allows for a maximum Rossby number of Ro ≈ -0.802 which is indeed slightly above the LLL, yet below the Keplerian value. Close to this critical point, the essential HMRI is then replaced by a helically modified SMRI. A third possibility arises by noting that the saturation of the MRI could lead to modified flow structures with parts of steeper shear, sandwiched with parts of shallower shear [21].

In this Letter, we discuss another promising way of extending the range of applicability of the inductionless versions of MRI to Keplerian profiles, and beyond. Rather than relying on modified electrical boundary conditions, or on locally steepened $\Omega(r)$ profiles, we will evaluate $B_\phi(r)$ profiles that are shallower than $1/r$. The main idea behind that is the following: assume that in a low-Pm region, characterized by $S \ll 1$ so that the standard MRI is reliably suppressed, Rm may still be sufficiently large for inducing azimuthal magnetic fields, either from a prevalent axial field B_z or by means of a dynamo process without any pregiven B_z. If B_ϕ is produced exclusively by an isolated axial current, we get $B_\phi \propto 1/r$. The other extreme case $B_\phi \propto r$ corresponds to the case of a homogeneous axial current density in the fluid which is already prone to the kink-type Tayler instability [22], even at Re = 0. For real accretion disks with complicated conductivity distributions in the radial and axial direction, quite a variety of intermediate $B_\phi(r)$ dependencies between $\propto 1/r$ and $\propto r$

profiles is well conceivable. Leaving those details aside, here we focus on the generic question of which deviations of the $B_\phi(r)$ profile from $1/r$ could make the HMRI (or AMRI) a viable mechanism for destabilizing Keplerian rotation profiles. By defining an appropriate magnetic Rossby number Rb we will show that the instability extends well beyond the LLL, even reaching Ro = 0 when going to Rb = -0.5. Evidently, in this extreme case of uniform rotation the only available energy source of the instability is the magnetic field. Most interestingly, by tracing the instability threshold further into the region of positive Ro in the Ro-Rb plane, we find a natural connection with the ULL whose meaning was a somewhat mysterious conundrum up to present.

We set out from the equations of incompressible, viscous, and resistive magnetohydrodynamics, i.e., the Navier-Stokes equation for the velocity field **u** and the induction equation for the magnetic field **B**, together with the continuity equation for incompressible flows and the divergence-free condition for the magnetic field:

$$\frac{\partial \mathbf{u}}{\partial t} + \mathbf{u} \cdot \nabla \mathbf{u} = \frac{\mathbf{B} \cdot \nabla \mathbf{B}}{\mu_0 \rho} - \frac{1}{\rho}\nabla\left(p + \frac{\mathbf{B}^2}{2\mu_0}\right) + \nu\nabla^2\mathbf{u}, \quad (1)$$

$$\frac{\partial \mathbf{B}}{\partial t} = \mathbf{B} \cdot \nabla \mathbf{u} - \mathbf{u} \cdot \nabla \mathbf{B} + \eta\nabla^2\mathbf{B}, \quad (2)$$

$$\nabla \cdot \mathbf{u} = 0, \qquad \nabla \cdot \mathbf{B} = 0. \quad (3)$$

We consider a purely rotational flow exposed to a magnetic field comprising a constant axial component and an azimuthal one with arbitrary radial dependence:

$$\mathbf{u}_0(r) = r\Omega(r)\mathbf{e}_\phi, \qquad \mathbf{B}_0(r) = B_\phi^0(r)\mathbf{e}_\phi + B_z^0\mathbf{e}_z. \quad (4)$$

To study flow and magnetic field perturbations on this background we linearize the equations in the vicinity of the stationary solution by assuming $\mathbf{u} = \mathbf{u}_0 + \mathbf{u}'$, $p = p_0 + p'$, and $\mathbf{B} = \mathbf{B}_0 + \mathbf{B}'$ and leaving only terms of first order with respect to the primed quantities. Introducing the total wave number $|\mathbf{k}|^2 = k_r^2 + k_z^2$, and $\alpha = k_z/|\mathbf{k}|$, where k_r and k_z are the radial and axial wave numbers of the perturbation, we define the viscous, resistive, and two Alfvén frequencies corresponding to B_z and B_ϕ:

$$\omega_\nu = \nu|\mathbf{k}|^2, \qquad \omega_\eta = \eta|\mathbf{k}|^2,$$
$$\omega_A = \frac{k_z B_z^0}{\sqrt{\rho\mu_0}}, \qquad \omega_{A_\phi} = \frac{B_\phi^0}{r\sqrt{\rho\mu_0}}. \quad (5)$$

Then, we define the ratio β of the two field components, a rescaled azimuthal wave number n, the Reynolds number Re, and the Hartmann number Ha as follows:

$$\beta = \alpha\frac{\omega_{A_\phi}}{\omega_A}, \qquad n = \frac{m}{\alpha},$$
$$\mathrm{Re} = \alpha\frac{\Omega}{\omega_\nu}, \qquad \mathrm{Ha} = \frac{\omega_A}{\sqrt{\omega_\nu\omega_\eta}}. \quad (6)$$

The steepness of $\Omega(r)$ will be measured by the hydrodynamic Rossby number, and the steepness of $B_\phi(r)$ by the corresponding magnetic Rossby number:

$$\text{Ro} = \frac{r}{2\Omega}\frac{\partial \Omega}{\partial r}, \qquad \text{Rb} = \frac{r}{2\omega_{A_\phi}}\frac{\partial \omega_{A_\phi}}{\partial r}. \qquad (7)$$

By employing the same short-wavelength (WKB) approximation as in Refs. [17,23], but now including Rb, we end up with a system of four coupled equations for the perturbations of arbitrary azimuthal wave number, yielding the ultimate dispersion relation $\det(M - \lambda I) = 0$, with λ denoting the (complex) growth rate in units of $\alpha\Omega$ and

$$M = \begin{pmatrix} -in - \frac{1}{\text{Re}} & 2\alpha & \frac{i\text{Ha}(1+n\beta)}{\sqrt{\text{ReRm}}} & \frac{-2\alpha\beta\text{Ha}}{\sqrt{\text{ReRm}}} \\ \frac{-2(1+\text{Ro})}{\alpha} & -in - \frac{1}{\text{Re}} & \frac{2\beta\text{Ha}(1+\text{Rb})}{\alpha\sqrt{\text{ReRm}}} & \frac{i\text{Ha}(1+n\beta)}{\sqrt{\text{ReRm}}} \\ \frac{i\text{Ha}(1+n\beta)}{\sqrt{\text{ReRm}}} & 0 & -in - \frac{1}{\text{Rm}} & 0 \\ \frac{-2\beta\text{Ha}\text{Rb}}{\alpha\sqrt{\text{ReRm}}} & \frac{i\text{Ha}(1+n\beta)}{\sqrt{\text{ReRm}}} & \frac{2\text{Ro}}{\alpha} & -in - \frac{1}{\text{Rm}} \end{pmatrix},$$

$$(8)$$

where $\text{Rm} = \text{RePm}$ is the magnetic Reynolds number. As a first test case, this relation can be applied to the kink-type Tayler instability that has recently been observed in a liquid metal experiment [22]. In the relevant limit with $\text{Pm} = 0$ and $\text{Re} = 0$ we deduce from the Bilharz criterion [24] the following condition for marginal stability:

$$\text{Rb} = \frac{(1 + \text{Ha}^2(n\beta + 1)^2)^2 - 4\text{Ha}^4\beta^2(n\beta + 1)^2}{4\text{Ha}^2\beta^2(1 + \text{Ha}^2(n\beta + 1)^2)}. \qquad (9)$$

For $\text{Rb} = 0$, which corresponds to $B_\phi \propto r$, and taking the limit $\beta \to \infty$, we obtain $\beta\text{Ha} = (1 - (1 \pm n)^2)^{-1/2}$, which would become equal to 1 for $n = \mp 1$. Translated to the real experiment with $k_z \approx 2.4/r$ and a very rough estimate $k_r \approx \pi/r$, we find a value of $\text{Ha}_{\text{exp}} := B_\phi(r)r\sqrt{\sigma/\rho\nu} \approx 34$ which is not too far from the experimentally observed value of 22 [22].

Our main focus here is, however, on the limit $\text{Re} \to \infty$ and $\text{Ha} \to \infty$ that is relevant for the MRI. Assuming for the moment $\text{Pm} = 0$ (which will be slightly relaxed later), and inserting the optimal relation between Re and Ha,

$$\text{Re} = 2\text{Rb}\sqrt{3\text{Rb} + 2}(\sqrt{1 + 2\text{Rb}} + \sqrt{2\text{Rb}})\beta^3\text{Ha}^3 \quad (10)$$

(obtained in the manner described in Ref. [17]), we find from the Bilharz criterion [24] the dependence of the critical Rossby number on Rb, n, and β:

$$\text{Ro}_{\text{cr}}^{\pm} = -2 + \frac{F \pm \sqrt{F^2 - 4\beta^2(n\beta + 1)^2}}{2\beta^2(n\beta + 1)^2}F, \qquad (11)$$

where $F = (n\beta + 1)^2 - 2\beta^2\text{Rb}$. Note that under the assumption $\text{Pm} = 0$ the dispersion relation possesses an exact solution, which after being expanded into the

Taylor series with respect to the interaction parameter $\text{N} = \text{Ha}^2\text{Re}^{-1}$ in the vicinity of $\text{N} = 0$ is

$$\lambda = -i(n \pm 2\sqrt{1 + \text{Ro}}) - \text{Re}^{-1}$$
$$- \text{N}\left(F \pm \frac{\beta(\text{Ro} + 2)(n\beta + 1)}{\sqrt{1 + \text{Ro}}}\right) + O(\text{N}^2). \quad (12)$$

At $n = 0$, $\text{Rb} = -1$, and $\text{Re} \to \infty$ the growth rates (12) reduce to those derived in Ref. [13]. In the limit $\text{N} \to 0$ and $\text{Re} \to \infty$ the stability boundary is obtained when the real part of the term linear in N vanishes. This condition leads exactly to Eq. (11), which also confirms the correct application of the Bilharz criterion.

With the goal to find extremal values of Ro that are compatible with marginal stability, we can further optimize β and n (or α) according to

$$\beta_{\text{opt}} = \frac{-1}{n \pm \sqrt{-2\text{Rb}}}, \qquad \alpha_{\text{opt}} = \left(m + \frac{\omega_A}{\omega_{A_\phi}}\right)\frac{\pm 1}{\sqrt{-2\text{Rb}}} \qquad (13)$$

to obtain $\text{Ro}_{\text{opt}}^{\pm}(\text{Rb}) = -2 - 4\text{Rb} \pm 2[2\text{Rb}(2\text{Rb} + 1)]^{1/2}$, or

$$\text{Rb} = -\frac{1}{8}\frac{(\text{Ro} + 2)^2}{\text{Ro} + 1}. \qquad (14)$$

Note that α_{opt} in Eq. (13) takes physically relevant values ($|\alpha_{\text{opt}}| < 1$) even for large enough $|m|$ if the sign of m is opposite to the sign of the ratio ω_A/ω_{A_ϕ} (cf. Ref. [17]). The relation (14), which is the central result of this Letter, is illustrated in Fig. 1. Let us start at the LLL, i.e., at $\text{Rb} = -1$, $\text{Ro}_{\text{LLL}} = \text{Ro}_{\text{opt}}^-(-1) \approx -0.828$. With increasing Rb, $\text{Ro}_{\text{opt}}^-(\text{Rb})$ also increases and reaches the Keplerian value $\text{Ro} = -3/4$ at $\text{Rb} = -25/32 = -0.78125$. At $\text{Rb} = -1/2$ we arrive at solid body rotation, i.e., $\text{Ro} = 0$. Interestingly, being connected at $\text{Rb} = -0.5$ to the branch $\text{Ro}_{\text{opt}}^+(\text{Rb})$ the threshold continues even into the positive Ro region corresponding to an outward increasing angular frequency. Finally it meets the ULL at $\text{Ro}_{\text{opt}}^+(-1) \approx +4.828$ when Rb comes back to -1.
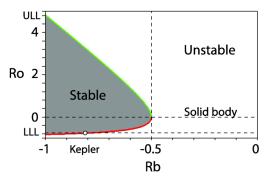

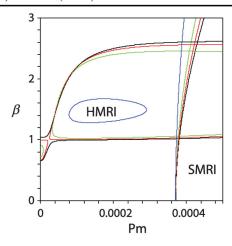FIG. 1 (color online). Dependence of the optimal critical Rossby numbers $\text{Ro}_{\text{opt}}^{\pm}$ on Rb when $\text{Pm} = 0$ and $\text{N} \to 0$.

P H Y S I C A L   R E V I E W   L E T T E R S

FIG. 2 (color). SMRI and HMRI for $n = 0$, $Ro = -3/4$, $Ha = 30$. Black: $Rb = -0.74$, $Re \approx 19876$. Red: $Rb = -0.75$, $Re \approx 21294$. Green: $Rb = -0.77$, $Re \approx 23935$. Blue: $Rb = -0.91$, $Re \approx 38553$. Middle of the blue loop: $Pm = 0.0002$, $S = HaPm^{1/2} \approx 0.42$, $Rm = RePm \approx 7.71$.

Having thus seen that HMRI can easily extend to Keplerian profiles, we still have to confirm that the shallow $B_\phi(r)$ profiles can indeed be produced by induction effects for which some finite value of Rm is still necessary. For the sake of illustration, we choose now $Ro_{Kep} = -3/4$, and $Ha = 30$. Figure 2 shows two groups of critical curves in the β-Pm plane. The four curves on the right side correspond to the SMRI; the curves continuing into the left part correspond to the HMRI. The latter ones consist, in general, of two parts, one reaching the inductionless $Pm = 0$ area. The connection between them typically happens at $Rm \approx 1$. In Figure 3 we show that this mechanism is not restricted to $n = m = 0$ but can easily extend to the range of the AMRI with higher azimuthal wave numbers m, both for small absolute values [see Fig. 3(a)] and large absolute values [see Fig. 3(b)] of β.

In summary, we have found that the range of applicability of the inductionless versions of the MRI that were previously thought to be restricted to $Ro < Ro_{LLL} \approx -0.828$ can easily extend to Keplerian profiles if only Rm is large enough to produce a $B_\phi(r)$ profile that is somewhat shallower than $1/r$. Interestingly, the $Ro_{opt}^+(Rb)$ curve starting with the ULL further continues to meet the $Ro_{opt}^-(Rb)$ branch at the solid body rotation. Since this extension of the inductionless forms of the MRI circumvents the usual demand $S \approx 1$, our finding may have significant consequences for the working of the MRI in the colder parts of accretion disks. A detailed investigation of the respective roles of S and Rm for the onset and the saturation mechanism of the instability in different astrophysical problems goes beyond the scope of this Letter and must be left for future work. We only note here that the sensitive structure of the instability domains in the low-Pm region, as seen in Figs. 2 and 3, may easily trigger a quasioscillatory behavior in the nonlinear regime. Our
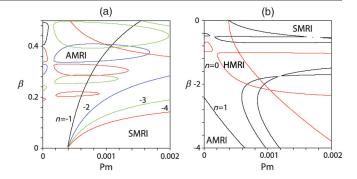

FIG. 3 (color). Domains of SMRI, HMRI, and AMRI for $Ha = 30$, $Ro = -3/4$, $Re = 4000$, $Rb = -0.755$, and (a) $n = -1$ (black), $n = -2$ (blue), $n = -3$ (green), $n = -4$ (red); and (b) $n = 0$ (red), and $n = 1$ (black).

results encourage experiments on the combination of the MRI and current driven instabilities as they are presently planned in the framework of the DRESDYN project [25].

*o.kirillov@hzdr.de
†f.stefani@hzdr.de

[1] S. A. Balbus and J. F. Hawley, Astrophys. J. **376**, 214 (1991).
[2] S. A. Balbus and P. Henri, Astrophys. J. **674**, 408 (2008).
[3] N. J. Turner and T. Sano, Astrophys. J. Lett. **679**, L131 (2008).
[4] W. Liu, J. Goodman, and H. Ji, Astrophys. J. **643**, 306 (2006).
[5] A. Brandenburg, A. Nordlund, R. F. Stein, and U. Torkelsson, Astrophys. J. **446**, 741 (1995).
[6] J. Herault, F. Rincon, C. Cossu, G. Lesur, G. I. Ogilvie, and P.-Y. Longaretti, Phys. Rev. E **84**, 036321 (2011).
[7] S. Fromang and J. Papaloizou, Astron. Astrophys. **476**, 1113 (2007).
[8] J. Shi, J. H. Krolik, and S. Hirose, Astrophys. J. **708**, 1716 (2010).
[9] P. J. Käpylä and M. J. Korpi, Mon. Not. R. Astron. Soc. **413**, 901 (2011).
[10] G. Lesur and P.-Y. Longaretti, Mon. Not. R. Astron. Soc. **378**, 1471 (2007).
[11] T. P. Fleming, J. M. Stone, and J. F. Hawley, Astrophys. J. **530**, 464 (2000); J. S. Oishi and M.-M. Mac Low, Astrophys. J. **740**, 18 (2011); M. Flock, T. Henning, and H. Klahr, Astrophys. J. **761**, 95 (2012).
[12] R. Hollerbach and G. Rüdiger, Phys. Rev. Lett. **95**, 124501 (2005).
[13] J. Priede, Phys. Rev. E **84**, 066314 (2011).
[14] W. Liu, J. Goodman, I. Herron, and H. Ji, Phys. Rev. E **74**, 056302 (2006).

[15] F. Stefani, G. Gerbeth, T. Gundrum, R. Hollerbach, J. Priede, G. Rüdiger, and J. Szklarski, Phys. Rev. E **80**, 066303 (2009).

[16] R. Hollerbach, V. Teeluck, and G. Rüdiger, Phys. Rev. Lett. **104**, 044502 (2010).

[17] O. N. Kirillov, F. Stefani, and Y. Fukumoto, Astrophys. J. **756**, 83 (2012).

[18] O. N. Kirillov and F. Stefani, Astrophys. J. **712**, 52 (2010).

[19] G. Rüdiger and R. Hollerbach, Phys. Rev. E **76**, 068301 (2007).

[20] O. N. Kirillov and F. Stefani, Phys. Rev. E **84**, 036304 (2011).

[21] O. M. Umurhan, Astron. Astrophys. **513**, A47 (2010).

[22] M. Seilmayer, F. Stefani, T. Gundrum, T. Weier, G. Gerbeth, M. Gellert, and G. Rüdiger, Phys. Rev. Lett. **108**, 244501 (2012).

[23] E. R. Krueger, A. Gross, and R. C. Di Prima, J. Fluid Mech. **24**, 521 (1966); M. J. Landman and P. G. Saffman, Phys. Fluids **30**, 2339 (1987); B. Eckhardt and D. Yao, Chaos Solitons Fractals **5**, 2073 (1995); S. Friedlander and M. M. Vishik, Chaos **5**, 416 (1995).

[24] H. Bilharz, Z. Angew. Math. Mech. **24**, 77 (1944).

[25] F. Stefani, S. Eckert, G. Gerbeth, A. Giesecke, Th. Gundrum, C. Steglich, T. Weier, and B. Wustmann, Magnetohydrodynamics **48**, 103 (2012).